

Simulation-driven Material Removal Compensation to Achieve Dimensional Accuracy after Abrasive Flow Machining

C.W. Kum¹, C.H. Wu², S. Wan²

¹Advanced Remanufacturing and Technology Centre, A*STAR, Singapore

²Institute of High Performance Computing, A*STAR, Singapore

kumcw@artc.a-star.edu.sg

Abstract

Abrasive flow machining (AFM) is a surface finishing process for internal channels based on extrusion of an abrasive-laden viscoelastic media. AFM can be applied on additive manufactured (AM) components such as nozzles, impellers and tool inserts to finish complex internal channels. However, due to high initial surface roughness of AM components (R_a 5 μm – 15 μm for laser sintering, R_a 30 μm – 100 μm for electron beam melting), substantial material removal (MR) is required for surface smoothing. As a result, final geometry after AFM may not meet the required dimensional accuracy. Further, MR distribution is dependent on the media flow field and therefore likely to be not uniform along the channel. The solution proposed and demonstrated in this work is ‘design for internal finishing’, where expected MR is compensated by adding materials during component design. The feasibility and advantage of this approach was demonstrated on a laser sintered test coupon resembling a nozzle guide vane (NGV) section. Firstly, to establish a baseline, AFM was applied on the original NGV design. Profile measurements of an NGV blade before and after AFM showed that dimensional error was almost 600 μm at some region of the blade profile. Then, based on the measured MR distribution, materials were added to a revised design of the blade, which was then fabricated. On this revised design, profile measurements before and after AFM showed that dimensional error was kept to within 200 μm . The proposed solution of MR compensation has thus been successfully demonstrated. Lastly, a computational fluid dynamics simulation of the AFM process and an MR model were also developed. MR distribution predicted by the simulation and MR model showed a good agreement with experimentally obtained MR distribution.

Abrasive flow machining, additive manufacturing, material removal, modelling, simulation

1. Introduction

Additive manufacturing (AM) has enabled the design and fabrication of components with complex internal geometry such as closed impellers, nozzles and mould inserts. However, rough as-printed surfaces (R_a 5 μm – 15 μm for laser sintering and R_a 30 μm – 100 μm for electron beam melting) may cause problems such as carbon deposition, corrosion and poor fatigue life, rendering the components unfeasible for actual applications [1].

One method to polish these internal channels is abrasive flow machining (AFM). During AFM, a viscoelastic abrasive-laden media is extruded through the internal channel, typically by a piston driven by hydraulics. As the media flows in the channel, abrasive particles in the media abrade the surface to remove material and improve surface roughness. The principles of AFM are illustrated in Figure 1, where a one-way flow configuration (common for complex component) is shown.

However, there are challenges when applying AFM on AM components. Due to high initial roughness of AM surfaces, the thickness of material that needs to be removed is significant (typically 5 times – 10 times the initial R_a). As a result, there may be a loss of dimensional accuracy after the AFM process. To compound the problem further, the material removal (MR) distribution depends on the media flow field during AFM and typically not uniform. This means that the final geometry after AFM will deviate from the target geometry in a manner that is difficult to predict and quantify.

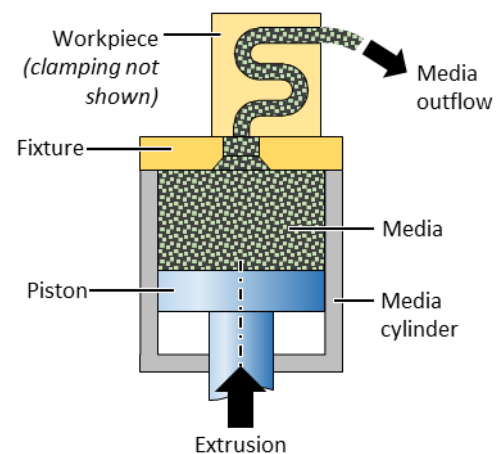


Figure 1. Illustration of the AFM process

A proposed solution is ‘design for internal finishing’, where expected material loss is compensated during component design by adding additional material to the component according to the predicted MR distribution. Efforts to predict MR distribution for AFM process have been reported in the literature [2, 3]. However, to the authors’ best knowledge, geometry modification based on predicted MR has not been demonstrated or reported so far. In this work, this approach of geometry modification for MR compensation is demonstrated on a laser sintered AM test coupon resembling a nozzle guide vane (NGV) section.

2. Experimental setup

In this section, the details of workpiece, fixture, AFM experimental conditions and measurement of MR by coordinate measurement machine (CMM) are described. Details on design revision and computational fluid dynamics simulation are given in a latter section.

2.1. Workpiece and fixture

The workpiece was a test coupon resembling a nozzle guide vane (NGV) section with five blades. It was built using a laser powder bed system (M 290, EOS) and material was MaragingSteel MS1 (EOS). Figure 2 below shows the photograph of a printed workpiece and also indicate the build direction.

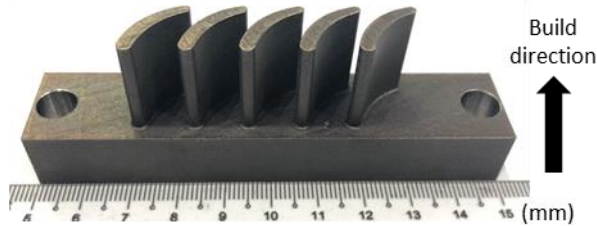


Figure 2. Photograph of NGV workpiece

Figure 3 below shows the schematic diagram and photograph of the fixture assembly. To form a closed passage for media flow, an enclosure was fabricated and attached to the workpiece. Then, the workpiece and enclosure were clamped between a pair of funnel plates and spacers. As the experiments were conducted on a large AFM system, support pillars were introduced to reduce clamping force on the workpiece.

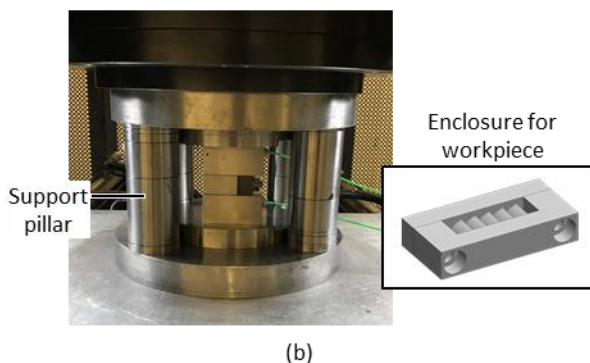
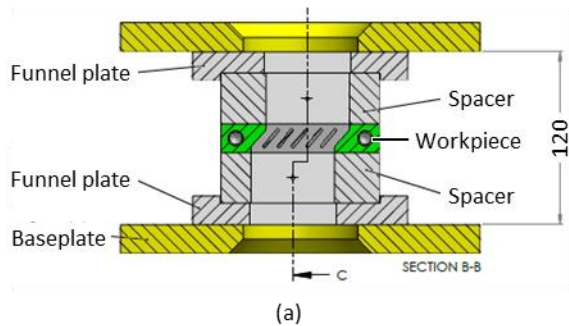


Figure 3. (a) Schematic diagram and (b) photograph of fixture assembly

2.2. AFM experimental conditions

Experiments were conducted on an industrial AFM system (EX4250, Extrude Hone Corporation). AFM media used was MV36 (Extrude Hone Corporation), classified as 'medium' viscosity and has silicon carbide abrasive particles of grit size #36 (about 700 μm median). Table 1 shows the experimental conditions, which were determined from preliminary trials.

Table 1 Experimental conditions of AFM process

Media cylinder diameter	150 mm
Media cylinder volume	5 L
Media type	MV36 (Extrude Hone Corp.)
Media grit size	#36
Extrusion pressure	10 MPa
Number of cycles	6

2.3. Measurement of MR

Profiles of the middle blade were measured using a coordinate measurement machine (ACCURA II, ZEISS). Three profiles at different heights were measured, as shown in Figure 4 below. Each profile consists of 1000 data points. These profiles were measured before and after the AFM process. Difference of the profiles gives the MR distribution.

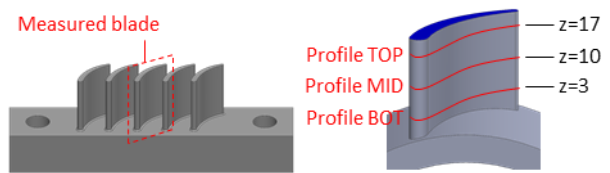


Figure 4. Schematic diagram of profiles measured by CMM

3. Results and discussion

3.1. Surface roughness after AFM

Surface roughness is not the focus of this work. Outside of this work, it has been demonstrated that R_a below 1 μm can be achieved for laser sintered surfaces. Photograph in Figure 5 shows the workpiece after AFM, where surface after AFM is visibly smooth.

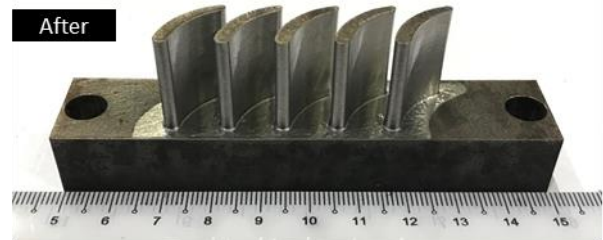


Figure 5. Photograph of workpiece after AFM

3.1. MR distribution for original design

Figure 6(a) shows the $z=10$ profile measured before and after AFM for the original design. It is apparent that the MR is not uniform, but instead higher at some regions of the blade profile. The MR distribution is quantified in Figure 6(b), which shows the dimensional error of each data point compared to the ideal CAD geometry. These errors were calculated by taking the Euclidean distance of associated pairs of data points before and after AFM.

In Figure 6(b), the red line shows that the dimensional error of as-printed geometry is within 200 μm across all data points. This matches the specifications given by the service bureau that fabricated the workpiece. However, after AFM, the dimensional error increased and almost reached 600 μm at the region of maximum error. From this, it is clear that even though surface roughness was improved after AFM, dimensional accuracy of the blade profile was lost.

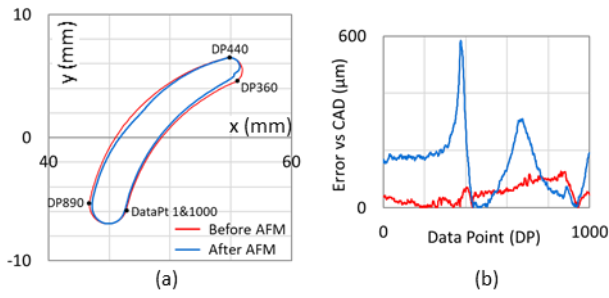


Figure 6. Original design, comparison before and after AFM for (a) blade profiles and (b) dimensional error against ideal CAD geometry

3.2. Design revision to compensate MR

Based on the measured MR distribution, the blade profile of the original design was revised. This was done by offsetting data points in the direction opposite of MR and with the same magnitude as measured MR. The revised design was fabricated in the same manner as the original design. Figure 7 below shows photographs of the blade profiles for the original and revised designs. It can be seen that the blade profile of the revised design is oversized to compensate for expected MR.

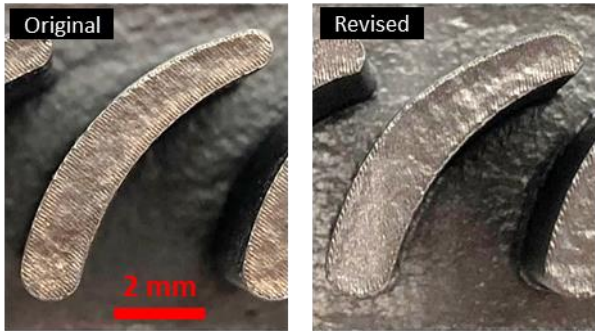


Figure 7. Blade profiles of original and revised designs

3.3. MR distribution for revised design

Figure 8(a) shows the comparison of blade profiles before and after AFM for the revised design. Before AFM, it can be seen that the blade profile is oversized according to the measured MR distribution in the original design. Figure 8(b) quantifies the dimensional error of the revised design after AFM. For the revised design, dimensional error is less than 200 μm after AFM for all data points, which is an improvement over the original design.

It is noted that the MR compensation did not eliminate dimensional error completely. There are two possible reasons for this. Firstly, there were dimensional errors associated with the as-built geometry that varies from part to part. MR compensation is not able or intended to eliminate this error. Secondly, geometry modification may affect the flow field of AFM media in the revised design. As such, MR distribution in the revised design will differ from the MR distribution in the original design. However, the effect is likely to be minimal for this specific geometry, given that MR is small (about 200 μm) relative to the size of the passage (about 3 mm). In cases where the change in MR distribution is significant, an iterative method to account for change of flow field is recommended for MR compensation.

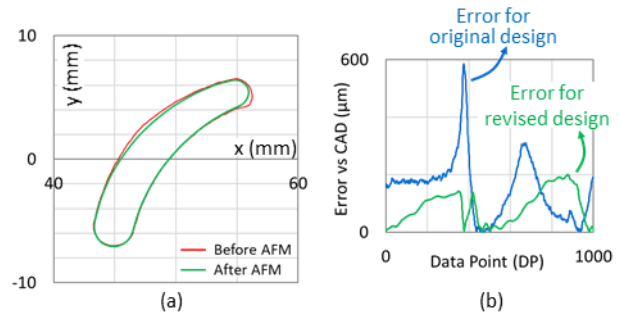


Figure 8. Revised design, (a) comparison of blade profiles before and after AFM and (b) comparison of dimensional error against ideal CAD geometry for original and revised design

4. Modelling and simulation

Although MR compensation has been demonstrated successfully, a scalable solution will necessitate that the MR distribution be determined without physical experiments. In this section, the measured MR distribution is compared against the results generated by a computational fluid dynamics (CFD) simulation and MR model developed outside of this work.

4.1. Simulation setup

The CFD simulation was conducted in OpenFOAM based on a previous development by the team. Figure 9 shows the fluid domain, which is the flow circuit bound by the fixture and workpiece. As indicated, there were two simulation runs – one for an up-flow condition and one for a down-flow condition. Flow direction is expected to affect flow field and MR distribution because the blade profile is not rotationally symmetrical. For AFM media, Phan-Thien-Tanner model was selected because AFM closely mirror an extrusion process. In the literature, other models such as Maxwell [4], power law [5] and $k-\epsilon$ turbulence [6, 7] have also been considered. Two separate simulations were conducted for each of the two flow directions. Table 2 shows the simulation conditions.

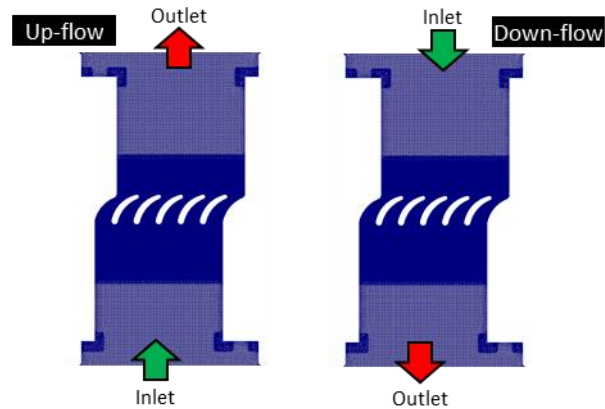


Figure 9. Simulation domain and media flow directions. Colour intensity corresponds to mesh density

Table 2 CFD simulation conditions

Software	OpenFOAM
Inlet boundary condition	Mass flow rate (0.4 kg/s)
Outlet boundary condition	Atmospheric pressure
Wall boundary condition	Full slip
Media model	Phan-Thien-Tanner
Number of grids	14 million

4.2. Comparison with experimental results

Figure 10 shows the comparison of MR distribution between experiment and simulation for one condition (up-flow, $z=10$). For simulation, the MR distribution was calculated by an MR model that considers a linear relationship between MR and the product of media velocity and total pressure. The MR distribution predicted by simulation is similar to the MR distribution obtained from experiments. This indicates that CFD simulation is a feasible alternative to physical experiments for obtaining MR distribution. This is critical for scaling this approach in the future.

For brevity, results for other conditions are not included but it is noted that similar agreement between simulation and experiment MR distributions were observed.

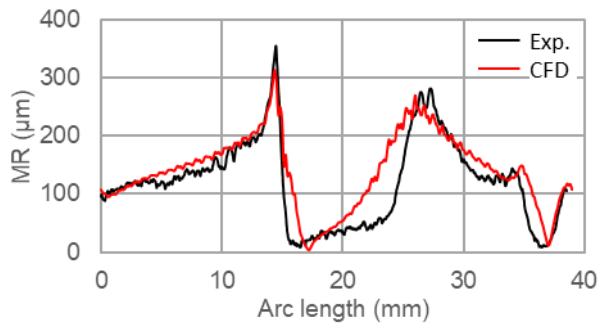


Figure 10. Comparison of MR distributions between experimental and simulation

5. Conclusion and future work

In this work, geometry modification to compensate for expected material removal (MR) has been demonstrated successfully on a laser sintered test coupon resembling a nozzle guide vane (NGV) section. Without MR compensation, dimensional error of blade profile (compared to CAD) was almost 600 μm at some regions after AFM. With MR compensation, dimensional error was reduced to within 200 μm for the whole blade profile. As a result, both surface roughness improvement and dimensional accuracy were achieved after AFM. Importantly, a CFD simulation and MR model developed outside of this work were able to accurately predict the MR distribution. Without the need to obtain MR distribution experimentally, there is potential for the solution to be applied at scale.

Two work strands are suggested for future work. Firstly, the approach demonstrated in this work can be extended to a full 3D internal passage, instead of a 2.5D structure used in this work. The methodology demonstrated in this work can be readily generalised to 3D geometry. Secondly, the approach demonstrated can be applied on smaller passages, where MR distribution will be significantly affected by the geometry change after MR compensation. In such cases, MR compensation through an iterative approach is recommended.

References

- [1] Frazier W 2014 Metal additive manufacturing: A review *J. Mater. Eng. Perform.* **23**(6) 1917–1928
- [2] Cheng K, Shao Y, Bodenhorst R and Jadva M 2017 Modelling and simulation of material removal rates and profile accuracy control in abrasive flow machining of the integrally bladed rotor blade and experimental perspectives *J. Manuf. Sci. Eng.* **139**(12) 121020
- [3] Shao Y and Cheng K 2019 Integrated modelling and analysis of micro-cutting mechanics with the precision surface generation in abrasive flow machining *Int. J. Adv. Manuf. Technol.* 1–13
- [4] Uhlmann E, Schmiedel C and Wendler J 2015 CFD simulation of the abrasive flow machining process *Procedia CIRP* **31**(6) 209–214

- [5] Wan S, Ang Y J, Sato T and Lim G C 2014 Process modelling and CFD simulation of two-way abrasive flow machining *Int. J. Adv. Manuf. Technol.* **71**(5–8) 1077–1086
- [6] Yuan Q L, Qi H and Wen D H 2016 Numerical and experimental study on the spiral-rotating abrasive flow in polishing of the internal surface of 6061 aluminium alloy cylinder *Powder Technol.* **302**(5) 153–159
- [7] Fu Y Z, Wang X P, Gao H, Wei H B and Li S C 2016 Blade surface uniformity of blisk finished by abrasive flow machining, *Int. J. Adv. Manuf. Technol.* **84**(5–8) 1725–1735